Molecular Vision 2007; 13:2282-2288 <http://www.molvis.org/molvis/v13/a258>
Received 15 September 2007 | Accepted 10 December 2007 | Published 17 December 2007

Sustained stress response after oxidative stress in trabecular meshwork cells

Guorong Li, Coralia Luna, Paloma B. Liton, Iris Navarro, David L. Epstein, Pedro Gonzalez

Department of Ophthalmology, Duke University, Durham, NC

Purpose: To investigate the mechanisms by which chronic oxidative stress may lead to a sustained stress response similar to that previously observed in the trabecular meshwork (TM) of glaucoma donors.
Methods: Porcine TM cells were treated with 200 μM H_2O_2 twice a day for four days and were allowed to recover for three additional days. After the treatment, TM cells were analyzed for generation of intracellular reactive oxygen species (iROS), mitochondrial potential, activation of NF-κB, and the expression of inflammatory markers IL-1α, IL-6, IL-8, and ELAM-1. Potential sources of iROS were evaluated using inhibitors for nitric oxide, nitric oxide synthetase, cyclooxygenase, xanthine oxidase, NADPH oxidase, mitochondrial ROS, and PKC. The role of NF-κB activation in the induction of inflammatory markers was evaluated using the inhibitors Lactacystin and BAY11–7082.
Results: Chronic oxidative stress simulated by H_2O_2 exposure of porcine TM cells resulted in the sustained production of iROS by the mitochondria. Inhibition of mitochondrial iROS had a significant inhibitory effect on the activation of NF-κB and the induction of IL-1α, IL-6, IL-8, and ELAM-1 triggered by chronic oxidative stress. Inhibition of NF-κB partially prevented the induction of IL-1α, IL-8, and ELAM-1, but not IL-6.
Conclusions: Chronic oxidative stress in TM cells induced iROS production in mitochondria. This increase in iROS may contribute to the pathogenesis of the TM in glaucoma by inducing the expression of inflammatory mediators previously observed in glaucoma donors as well as the levels of oxidative damage in the tissue.

Glaucoma is a major cause of irreversible blindness, affecting more than70 million individuals worldwide [1]. Elevated intraocular pressure (IOP) is a major risk factor in the development of glaucoma [2] and in the progression of glaucomatous damage [3]. High IOP usually occurs as a result of an increase in aqueous humor outflow resistance in TM. The specific mechanisms leading to the failure of the TM to maintain normal levels of aqueous humor outflow resistance are not yet understood.

It has been reported that glaucoma is characterized by the sustained activation of a tissue-specific stress response in the cells of the TM. Such a stress response includes the sustained activation of NF-κB and the expression of inflammatory markers such as interleukin (IL)-1α and vascular endothelial leukocyte-adhesion molecule (ELAM)-1 [4]. It has been recently reported that treatment of porcine TM cells with an acute treatment with H_2O_2 (1 mM concentration) induces the expression of ELAM-1 [5], suggesting that oxidative stress could contribute to the expression of this protein in POAG. A contributing role for oxidative stress in the morphologic and physiologic alterations in the aqueous outflow pathway in aging and glaucoma has been hypothesized for a long time and is supported by some experimental evidence [6-16].

Correspondence to: Dr. Pedro Gonzalez, Department of Ophthalmology, Duke University Medical Center, Erwin Rd., Box 3802, Durham, NC, 27710; Phone: (919) 681 5995; FAX: (919) 684 8983; email: gonza012@mc.duke.edu

Sublethal oxidative damage has been shown to result in the induction of inflammatory markers in several cell types [17-19]. Sublethal oxidative damage has also been shown to lead to a prolonged increase in the endogenous generation of iROS in several cell types [20-23]. An increase in iROS generation has the potential to result in sustained activation of NF-κB, which is likely to induce the expression of proinflammatory markers. Therefore, we investigated whether chronic oxidative stress in TM cells can lead to increased production of iROS and whether, in turn, this would result in sustained activation of a stress response involving sustained activation of NF-κB and the expression of inflammatory markers similar to that observed in POAG. We also analyzed the potential sources of iROS generation induced by chronic oxidative stress in porcine TM cells.

METHODS

Porcine trabecular meshwork cell culture: TM tissue from fresh porcine eyes was digested in 10 mg collagenase/20 mg BSA (BSA)/5 ml phosphate buffer saline (PBS) solution. The cells were plated on gelatin coated 10 cm Petri dishes and maintained at 37 °C in a humidified atmosphere of 5% CO2 in TM culture medium. The TM culture medium was low glucose Dulbecco's Modified Eagle Medium (DMEM) with L-glutamine and 110 mg/l sodium pyruvate, supplemented with 10% fetal bovine serum (FBS), 100 μM nonessential amino acids, 100 units/ml penicillin, and 100 μg/ml streptomycin sulfate. All reagents were obtained from Invitrogen Corporation (Carlsbad, CA).

Table 1. Primer sequences used for real-time quantitative polymerase chain reaction analysis.

Gene	Accession number	Forward primer	Reverse primer
IL-1a	NM_214029	AAGTGTTGACAGGCCGTATG	TACCAGACTTCGCTCCCTCT
ELAM-1	NM_214268	CCCATGGAACACAACCTGTGCATT	AGCTTTACACGTTGGCTTCTTGCC
IL-8	AB057440	AAACTGGCTGTTGCCTTCTT	ATTTATGCACTGGCATCGGAA
IL-6	NM_214399	GCTTCCAATCTGGGTTCAAT	CTAATCTGCACAGCCTCGAC
b-actin	AY550069	AAGATCAAGATCATCGCGCCTCCA	TGGAATGCAACTAACAGTCCGCCT

For each gene, the nucleotide sequences of the two specific primers were detailed. The gene accession number used to find both primers is indicated. Abbreviations are: IL-1α, interleukin-1 alpha; ELAM-1, vascular endothelial leukocyte-adhesion molecule-1; IL-8, interleukin-8; and IL-6, interleukin-6.

Chemicals: Lactacystin (Lact, L6785), BAY11–7082 (BAY, B5556), Dibenziodolium chloride (DPI, D2926), Oxypurinol (Oxy, O4502), Indomethacin (Indo, I7378), /N/ω-Nitro-L-arginine methyl ester hydrochloride (L-NAME, N5751), Apocynin (Apo, A10809), Aminoguanidine bicarbonate salt (AMG, A7259), Carbonyl cyanide 4-(trifluoromethoxy) phenylhydrazone (Fccp, C2920), Chelerythrine Chloride (Chele, C2932), and 30% Hydrogen peroxide solution (H_2O_2, 31642) were commercially obtained from Sigma-Aldrich (St. Louis, MO). 5,5′,6,6'-tetrachloro-1, 1',3,3′-tetracthylbenzimidazolylcarbocyanine iodide (JC-1, M34152) and 2',7'-dichlorodihydrofluorescein diacetate (H_2DCFDA, D-399) were purchased from Molecular Probes (Carlsbad, CA).

H_2O_2 treatment: Porcine TM cells (passage 4–5) were treated with H_2O_2 200 \mu M in DMEM containing 10% FBS, twice a day, for four days. To differentiate from acute stress responses to oxidative challenge, TM cells were allowed a recovery time of three days after the H_2O_2 treatment. The medium was changed with fresh DMEM containing 10% FBS on the first recovery day. For iROS assay, inhibitors were pretreated 1 h in a serum free condition followed by H_2DCFDA incubation. For realtime Q-PCR and NF-κB activity assay, inhibitors were used 24 h before RNA and protein extractions. For IL-6 and IL-8 ELISA assay, supernatant was collected at the end of the recovery day.

Preparation of cytosolic and nuclear extracts: Cells were trypsinized and washed twice with cold PBS and lysed with 200 µl cytosolic lysis buffer (10 mM Tris-HCl [pH7.4], 10 mM NaCl, 3 mM $MgCl_2$, 0.5% NP-40, 1 mM dTT, and freshly added proteinase inhibitor cocktail), incubated on ice for 15 min and vortexed 10 s. Cytosolic proteins were collected after centrifugation at 1,500× g for 5 min at 4 °C. The pellet was washed once with wash buffer (20 mM Hepes, pH 7.9, 1.5 mM $MgCl_2$, and 0.2 mM EDTA), resuspended with nuclear lysis buffer (20 mM Hepes, pH 7.9, 25% glycerol, 0.42 M NaCl, 1.5 mM $MgCl_2$, 0.2 mM EDTA with freshly added protease inhibitor cocktail), and shaken in an orbital shaker for 30 min at 4 °C. Nuclear proteins were collected after centrifugation at 10,000× g for 10 min at 4 °C. Protein concentration was measured using the Micro BCA Protein assay kit (23235; Pierce, Rockford, IL) following the instruction.

NoShift II NF-κB assay: Nuclear NF-κB activities were determined with the NoShift II Transcription Factor (71680–3; Novagen, Inc., Madison, WI) following the manufacturer's instructions. Briefly, 3 µg of nuclear protein was mixed with Binding solution and incubated for 20 min at RT. Following additional incubation with Binding Reagent for 20 min at RT, digestion buffer or Digestion Reagent was added to each reaction. The reaction mixtures were incubated at 37 °C for 20 min and then transferred to NoShift II Capture Plate for a 45 min hybridization period at RT with vigorous shaking. After washing four times with Wash Buffer, Detection Reagent was added to each well and the plate was incubated 30 min at RT with shaking. Following a second set of four washes, Chemiluminescent Substrate was added to each well and incubated 30 min at 37 °C. Light intensity was then measured with a microplate chemiluminometer, and the results were adjusted for negative control reading and recorded as relative light units (RLUs).

RNA extraction and real-time quantitative polymerase chain reaction: Total RNA from porcine TM cells was isolated using the RNeasy kit (Qiagen Inc., Valencia, CA) following the manufacturer's protocol. First strand cDNA was synthesized using oligodT primer and Superscript II reverse transcriptase (Invitrogen, Carlsbad, CA) according to the manufacturer's instructions. Real-time Q-PCR was performed using iQ SYBR Green Supermix (BioRad, Hercules, CA) in the BioRad iCycler iQ system (BioRad, Hercules, CA). Fold expression changes were determined using the iCycle iQ system software. β-Actin served as an internal standard of mRNA expression. The sequences of the primers used for the amplifications are indicated in Table 1.

Assay of iROS: The production of iROS was measured by DCFH oxidation as described previously, with minor modifications [24]. Briefly, 10 mM H_2DCFDA was dissolved in methanol and was diluted 500 fold in HBSS to give a 20 µM concentration of H_2DCFDA. H_2O_2 treated and control cells in 96-well plates were treated with inhibitors and their specific vehicles for 1 h, and then exposed to H_2DCFDA for an additional 1 h. After incubation, the fluorescence was read

at 485 nm excitation and 530 nm emission on a fluorescence plate reader.

Measurement of mitochondrial membrane potential ($\Delta\psi_m$): Mitochondrial membrane potential was monitored in cells loaded with 2 µM of JC-1 dye according to the manufacturer instructions. JC-1 is a positively charged fluorescent compound, which is taken up by mitochondria proportionally to the inner mitochondrial membrane potential. When a critical concentration is reached, JC-1 monomers (fluorescent green) form aggregates (fluorescent red). Briefly, cells in six-well plates treated with or without H_2O_2 were trypsinized and pellet by centrifuge. The cells were then washed with PBS once, loaded with JC-1 in 1 ml of PBS to final concentration of 2 µM, and incubated at 37 °C, 5% CO_2 for 15 min. The cells were pelleted and washed again with PBS, then resuspended in 200 µl of PBS. The cells were analyzed on a flow cytometer with 488 nm excitation using emission filters appropriate for Alexa Fluor 488 dye and R-phycoerythrin.

Quantification of cytokines by enzyme-linked immunosorbent assay (ELISA): IL-6 and IL-8 protein levels in cell culture supernatant were determined using the Quantikine porcine ELISA kits (P6000 and P8000; R&D Systems, Minneapolis, MN) according to the manufacturer's instructions. The optical density was read using a microplate reader setting to 450 nm with 540 nm correction.

Statistical analysis: The data were presented as the mean ±SD. For multiple comparisons of groups, ANOVA was used. Statistical significance between groups was assessed by paired or unpaired Student's *t* test, with Bonferroni's correction. A value of $p<0.05$ was considered statistically significant.

RESULTS

Chronic oxidative stress induced the activation of NF-κB and upregulation of inflammatory markers IL-6, ELAM-1, IL-1α, and IL-8: As indicated in Methods, TM cells were treated with H_2O_2 (200 µM) twice a day for four days and then they were allowed three days of recovery. After this treatment, TM cells showed a fourfold increase ($p<0.01$, compared to control) in the levels of activation of NF-κB analyzed by NoShift II NF-κB Assay (Figure 1A). The activation of NF-κB was accompanied by a significant upregulation of inflammatory mediators including IL-6, ELAM-1, IL-1α, and IL-8 (Figure 1B,C).

Oxidative stress results in increased production of iROS and loss of $\Delta\psi_m$: As shown in Figure 1D, cells subjected to oxidative stress showed a significant ($p<0.01$) increase of 25% in iROS production measured with H_2DCFDA. This increase in iROS generation was accompanied by a significant ($p<0.01$) decrease of 30% in mitochondrial membrane potential measured by JC-1 (Figure 1D).

Sources of iROS production after oxidative stress: Inhibition of nitric oxide with L-NAME, nitric oxide synthetase with AMG, cyclooxygenase (COX) with Indo, and xanthine oxidase with Oxy, did not have any significant effect on the induction of iROS (Figure 2A). The NADPH oxidase inhibitor DPI and the PKC inhibitor Chele exerted some inhibitory effect on the total iROS in a dose dependent manner (14%, 25%, and 34% for Chele, and 9%, 13%, and 28% for DPI; $p<0.05$ and 0.01; Figure 2B,C). The highest effect on iROS production was obtained by inhibiting mitochondrial ROS generation with Fccp (45%, 49%, and 51% reduction; $p<0.001$; Figure 2D).

Effect of PKC inhibition on the induction of iROS: The PKC inhibitor, Chele showed some effect on the production of iROS (Figure 2B). However, Chele did not have any significant effect on the induction of IL-6, IL-8, IL-1α, and ELAM-1 (data not shown).

Role of iROS in induction of NF-κB, IL-6, ELAM-1, IL-1α, and IL-8: Inhibition of iROS production by Fccp had a significant effect on the reduction of NF-κB activities (43.3%, $p<0.01$), as well as on the decrease of IL-6 (49.3%, $p<0.01$), ELAM-1 (84.2%, $p<0.001$), IL-1α (67.3%, $p<0.01$) and IL-8 (98.1%, $p<0.01$) after oxidative stress (Figure 3).

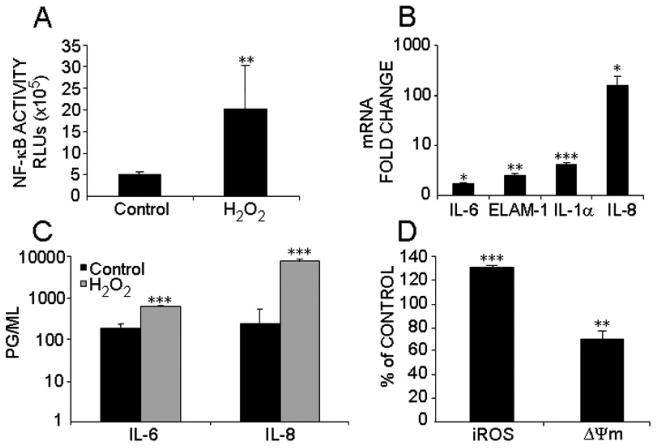

Figure 1. Induction of proinflammatory factors by chronic H_2O_2 treatment. TM cells were treated with H_2O_2 200 µM twice a day for four days and then they were allowed three days to recover. **A**: Activation of NF-κB measured by NoShift II NF-κB assay. Data represents the mean values of NF-κB activation in relative light units (rlu) ±SD of n=3. **B**: Realtime Q-PCR analysis of the induction of IL-1α, IL-6, IL-8, and ELAM-1. For each individual sample, the expression level of each gene was first normalized with that of β-actin and then the relative differences between groups were expressed as mean fold changes compared with the controls ±SD of n=3. **C**: Protein levels of IL-6 and IL-8 in cell culture media assessed by ELISA. Data represent means of protein concentration ±SD of n=6. **D**: Induction of iROS and decrease of $\Delta\psi_m$ detected by H_2DCFDA and JC-1. Data showed a percentage of control ±SD (n=5) in iROS treated with H_2O_2. This increase in iROS was associated with a reduction of percentage ±SD in $\Delta\psi_m$ (n=3). An asterisk means that $p<0.05$; a double asterisk means that $p<0.01$; and three asterisks mean that $p<0.001$ (compared to nontreated control).

NF-κB activation is involved in the induction of ELAM-1, IL-1α, and IL-8: The two NF-κB inhibitors tested (Lact 10 μM and BAY 5 μM) significantly decreased the induction of ELAM-1 (Lact: 36.2%, $p<0.05$; BAY: 44.4%, $p<0.01$) and IL-1α (Lact: 55.9%, $p<0.01$; BAY: 40%, $p<0.05$). BAY significantly reduced IL-8 expression, but Lact did not (Lact: 27.6%, $p=0.07$; BAY: 88.8%, $p<0.01$). However, none of the NF-κB inhibitors had any significant effect on the induction of IL-6 after oxidative stress (Figure 4).

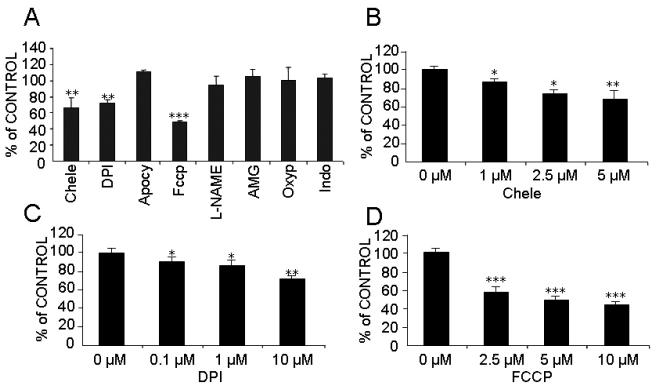

Figure 2. Sources of iROS in pTM cells induced by H_2O_2 treatment. Production of iROS after H_2O_2 treatment was determined by H_2DCFDA. **A**:The following inhibitors were added to the cultures 1 h before H_2DCFDA incubation: Chele; 5 μM, DPI; 10 μM, Apo; 10 μM, Fccp; 10 μM, L-NAME; 1 mM, AMG; 10 μM, Oxyp; 20 μM, and Indo; 200 μM. The data represent the mean ±SD (n=3) of iROS percentage change treated with inhibitors compared to controls treated with the same vehicles in which the inhibitors were prepared. Additional experiments were conducted to evaluate the dose response to Chele (**B**), DPI (**C**), and Fccp (**D**). An asterisk means $p<0.05$; a double asterisk means $p<0.01$; and three asterisks mean $p<0.001$ (n=3).

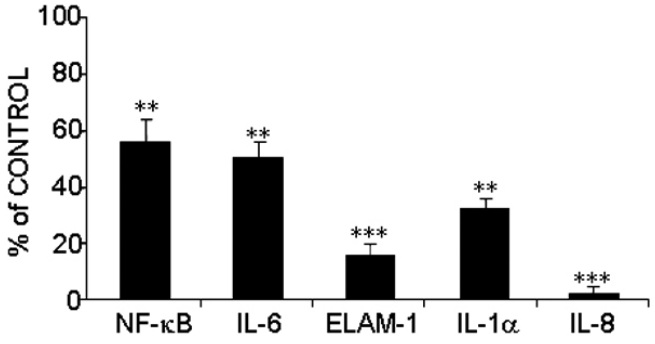

Figure 3. Role of iROS generation in the induction of NF-κB and proinflammatory mediators. The activation of NF-κB measured by the NoShift II NF-κB assay and the induction of IL-6, IL-8, IL-1α, and ELAM-1 measured by real-time Q-PCR, were evaluated in pTM cells treated with H_2O_2 in the presence or absence of 5 μM Fccp. The data show percentage changes in cultures treated with Fccp and H_2O_2 compared to those treated with vehicle (ethanol) and H_2O_2. A double asterisk means $p<0.01$; three asterisks mean $p<0.001$ (n=3).

DISCUSSION

In the present study, we found that chronic H_2O_2 treatment resulted in sustained activation of NF-κB and the upregulation of proinflammatory markers, including ELAM-1, IL-1α, IL-6, and IL-8. Our data shows that chronic H_2O_2 treatment resulted in increased generation of iROS, a key mediator of the observed activation of NF-κB and the induction of inflammatory mediators. A similar increase in iROS production after exogenous H_2O_2 treatment has been observed in several cell types [20-22,25] and appears to be a feature of sublethal damaged and senescent cells [20]. Different mechanisms have been implicated in the endogenous generation of ROS after an oxidative stress challenge. These mechanisms include the activation of NADPH oxidase (NOX) [21] to produce anion superoxide radical (O^{2-}) [21,25], intracellular mitochondrial H_2O_2 generation [22], xanthine oxidase [26], uncoupled endothelial nitrite oxide synthase (eNOS) [27], and COX [28].

The observed lack of effect of the inhibitors for xanthine oxidase with Oxy, eNOS with L-NAME, AMG, and COX with Indo, suggests that none of these enzymes may contribute significantly to the increase in iROS production after oxidative challenge in TM cells.

The induction of iROS was partially inhibited by the NOX inhibitor DPI. DPI is a large spectrum inhibitor of electron transporters including not only various NOX enzymes, but also mitochondrial oxidase and xanthine oxidase [29]. Therefore, the effects of DPI could potentially be attributed to inhibitory effects on mitochondrial and xanthine

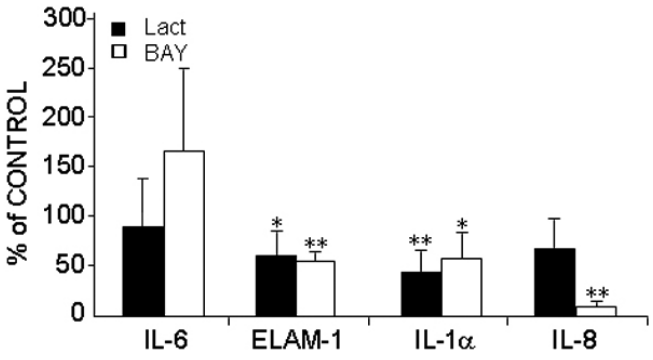

Figure 4. Role of NF-κB activation in the induction of proinflammatory mediators. The levels of induction of IL-6, IL-8, IL-1α, and ELAM-1 three days after H_2O_2 treatment were evaluated by realtime Q-PCR in the presence or absence of the NF-κB inhibitors Lact 10 μM and BAY 5 μM. The data show percentage changes in cultures treated with NF-κB inhibitors (Lact and BAY) and H_2O_2 compared to those treated with vehicle (DMSO) and H_2O_2. An asterisk means $p<0.05$; a double asterisk means $p<0.01$ (n=3–4).

oxidase ROS production. However, since the inhibitor of xanthine oxidase, Oxy, did not have any effect on iROS generation, it is unlikely that the effect observed with DPI would result from xanthine oxidase inhibition. Similarly, the inhibitory effects of DPI on iROS generation can not be attributed to mitochondrial inhibition since inhibition of ROS generation occurred in the submicromolar range, while DPI inhibition of mitochondrial oxidase occurs with an IC_{50} of approximately 10 μM DPI [30,31]. In addition, while inhibition of iROS generation by the mitochondrial inhibitor Fccp also blocked the activation of NF-κB and upregulation of proinflammatory markers, treatment with DPI had no significant effect in any of these variables. In comparison with DPI, the NOX inhibitor Apo did not have any effect on iROS induction. This result is not necessarily surprising since Apo is known to require myeloperoxidase-dependent metabolism for full activity and therefore does not effectively inhibit NOX activity in all cell types [32]. Therefore, our data suggests that H_2O_2 treatment may lead to some activation of NOX that should contribute to the total increase in ROS generation, but is not responsible for the sustained activation of NF-κB and the expression of inflammatory markers. In contrast, the mitochondrial inhibitor Fccp, which is a protonophore (H^+ ionophore) and uncoupler of oxidative phosphorylation in mitochondria, was capable of reducing iROS production in a dose-dependent manner. Treatment with Fccp inhibited the induction of NF-κB, IL-1α, IL-6, IL-8, and ELAM-1, suggesting that the production of iROS by the mitochondria plays a key role in the activation of NF-κB and proinflamatory markers that result from chronic oxidative stress in TM cells.

The activation of NF-κB appears to mediate the induction of IL-1α, IL-8, and ELAM-1, but not that of IL-6. Our results showed that neither of the two NF-κB inhibitors tested had any effect on IL-6 induction after oxidative stress. Therefore, endogenous ROS may activate other pathways different from NF-κB that also contribute to the induction of inflammatory mediators after oxidative stress including the induction of IL-6.

PKC has been implicated in the activation of iROS production by NOX and mitochondria in several cell types [33-35]. Treatment of TM cells with Chele, a PKC inhibitor, resulted in partial inhibition of iROS generation with no effect observed on the induction of inflammatory markers. Therefore, although activation of PKC might contribute to the induction of iROS production, it does not appear to be the exclusive mechanism leading to iROS generation and is not necessary to activate the induction of inflammatory mediators. Therefore, alternative mechanisms should be involved in the activation of iROS generation.

It has been proposed that while short-term activation of inflammatory mediators such as IL-1α and IL-6 may help to decrease IOP [36,37], their chronic activation may exert pathologic affects on the TM and contribute to the progression of glaucoma [38]. Therefore, the observed induction of iROS production resulting form oxidative stress may constitute mechanisms by which oxidative stress could contribute to the pathogenesis of glaucoma through the sustained activation of inflammatory mediators.

In addition to the upregulation of proinflammatory cytokines, the observed induction of iROS after chronic oxidative stress also has the potential to contribute by itself to pathophysiological changes of the outflow pathway by increasing the levels of oxidative damage in the cells. Consistent with this concept, our data showed a decrease in mitochondria potential following this chronic H_2O_2 treatment (Figure 2). Furthermore, the mitochondria damage and generation of the secondary ROS was persistent since loss of mitochondria potential is irreversible by Fccp (data not shown).

In summary, our results show that chronic oxidative stress leads to the endogenous production of ROS by the mitochondria in TM cells, which in turn induces a sustained stress response characterized by activation of NF-κB and expression of inflammatory markers. The endogenous production of ROS by TM cells resulting from oxidative stress might thus contribute to the pathogenesis of the TM in glaucoma by inducing the expression of inflammatory mediators previously observed in the TM of glaucoma donors and by increasing the levels of oxidative damage in the tissue.

ACKNOWLEDGMENTS

This work was supported by NEI EY01894, NEI EY016228, NEI EY05722, and Research to Prevent Blindness. We also gratefully thank Dr. Ping Yang's technical support for this project.

REFERENCES

1. Quigley HA. Number of people with glaucoma worldwide. Br J Ophthalmol 1996; 80:389-93. [PMID: 8695555]
2. Kass MA, Heuer DK, Higginbotham EJ, Johnson CA, Keltner JL, Miller JP, Parrish RK 2nd, Wilson MR, Gordon MO. The Ocular Hypertension Treatment Study: a randomized trial determines that topical ocular hypotensive medication delays or prevents the onset of primary open-angle glaucoma. Arch Ophthalmol 2002; 120:701-13. [PMID: 12049574]
3. Heijl A, Leske MC, Bengtsson B, Hyman L, Bengtsson B, Hussein M, Early Manifest Glaucoma Trial Group. Reduction of intraocular pressure and glaucoma progression: results from the Early Manifest Glaucoma Trial. Arch Ophthalmol 2002; 120:1268-79. [PMID: 12365904]
4. Wang N, Chintala SK, Fini ME, Schuman JS. Activation of a tissue-specific stress response in the aqueous outflow pathway of the eye defines the glaucoma disease phenotype. Nat Med 2001; 7:304-9. [PMID: 11231628]
5. Zhou Q, Liu YQ, Zhao JL, Zhang H. Effects of oxidative stress on the expression of endothelial-leukocyte adhesion molecule-1 in porcine trabecular meshwork cells. Zhongguo Yi Xue Ke Xue Yuan Xue Bao 2007; 29:394-7. [PMID: 17633469]

6. Alvarado J, Murphy C, Polansky J, Juster R. Age-related changes in trabecular meshwork cellularity. Invest Ophthalmol Vis Sci 1981; 21:714-27. [PMID: 7298275]
7. Alvarado J, Murphy C, Juster R. Trabecular meshwork cellularity in primary open-angle glaucoma and nonglaucomatous normals. Ophthalmology 1984; 91:564-79. [PMID: 6462622]
8. Zhou L, Li Y, Yue BY. Oxidative stress affects cytoskeletal structure and cell-matrix interactions in cells from an ocular tissue: the trabecular meshwork. J Cell Physiol 1999; 180:182-9. [PMID: 10395288]
9. Kahn MG, Giblin FJ, Epstein DL. Glutathione in calf trabecular meshwork and its relation to aqueous humor outflow facility. Invest Ophthalmol Vis Sci 1983; 24:1283-7. [PMID: 6885312]
10. De La Paz MA, Epstein DL. Effect of age on superoxide dismutase activity of human trabecular meshwork. Invest Ophthalmol Vis Sci 1996; 37:1849-53. [PMID: 8759353]
11. Freedman SF, Anderson PJ, Epstein DL. Superoxide dismutase and catalase of calf trabecular meshwork. Invest Ophthalmol Vis Sci 1985; 26:1330-5. [PMID: 4044161]
12. Tan JC, Peters DM, Kaufman PL. Recent developments in understanding the pathophysiology of elevated intraocular pressure. Curr Opin Ophthalmol 2006; 17:168-74. [PMID: 16552252]
13. Gabelt BT, Kaufman PL. Changes in aqueous humor dynamics with age and glaucoma. Prog Retin Eye Res 2005; 24:612-37. [PMID: 15919228]
14. Kumar DM, Agarwal N. Oxidative stress in glaucoma: a burden of evidence. J Glaucoma 2007; 16:334-43. [PMID: 17438430]
15. Izzotti A, Sacca SC, Cartiglia C, De Flora S. Oxidative deoxyribonucleic acid damage in the eyes of glaucoma patients. Am J Med 2003; 114:638-46. [PMID: 12798451]
16. Saccà SC, Pascotto A, Camicione P, Capris P, Izzotti A. Oxidative DNA damage in the human trabecular meshwork: clinical correlation in patients with primary open-angle glaucoma. Arch Ophthalmol 2005; 123:458-63. [PMID: 15824217]
17. Shimada T, Watanabe N, Hiraishi H, Terano A. Redox regulation of interleukin-8 expression in MKN28 cells. Dig Dis Sci 1999; 44:266-73. [PMID: 10063910]
18. Verhasselt V, Goldman M, Willems F. Oxidative stress up-regulates IL-8 and TNF-alpha synthesis by human dendritic cells. Eur J Immunol 1998; 28:3886-90. [PMID: 9842932]
19. Josse C, Boelaert JR, Best-Belpomme M, Piette J. Importance of post-transcriptional regulation of chemokine genes by oxidative stress. Biochem J 2001; 360:321-33. [PMID: 11716760]
20. Zdanov S, Remacle J, Toussaint O. Establishment of H2O2-induced premature senescence in human fibroblasts concomitant with increased cellular production of H_2O_2. Ann N Y Acad Sci 2006; 1067:210-6. [PMID: 16803987]
21. Li WG, Miller FJ Jr, Zhang HJ, Spitz DR, Oberley LW, Weintraub NLH. (2)O(2)-induced O(2) production by a non-phagocytic NAD(P)H oxidase causes oxidant injury. J Biol Chem 2001; 276:29251-6. [PMID: 11358965]
22. Tampo Y, Kotamraju S, Chitambar CR, Kalivendi SV, Keszler A, Joseph J, Kalyanaraman B. Oxidative stress-induced iron signaling is responsible for peroxide-dependent oxidation of dichlorodihydrofluorescein in endothelial cells: role of transferrin receptor-dependent iron uptake in apoptosis. Circ Res 2003; 92:56-63. [PMID: 12522121]
23. Li PC, Li SC, Lin YJ, Liang JT, Chien CT, Shaw CF. Thoracic vagal efferent nerve stimulation evokes substance P-induced early airway bronchonstriction and late proinflammatory and oxidative injury in the rat respiratory tract. J Biomed Sci 2005; 12:671-81. [PMID: 16078002]
24. Li G, Cui G, Tzeng NS, Wei SJ, Wang T, Block ML, Hong JS. Femtomolar concentrations of dextromethorphan protect mesencephalic dopaminergic neurons from inflammatory damage. FASEB J 2005; 19:489-96. [PMID: 15790998]
25. Seshiah PN, Weber DS, Rocic P, Valppu L, Taniyama Y, Griendling KK. Angiotensin II stimulation of NAD(P)H oxidase activity: upstream mediators. Circ Res 2002; 91:406-13. [PMID: 12215489]
26. Ohta Y, Matsura T, Kitagawa A, Tokunaga K, Yamada K. Xanthine oxidase-derived reactive oxygen species contribute to the development of D-galactosamine-induced liver injury in rats. Free Radic Res 2007; 41:135-44. [PMID: 17364939]
27. Kondoh K, Matsushiro N, Satoh T, Kuramasu T, Kubo T. Audiological effect of bone-anchored hearing aid. Nippon Jibiinkoka Gakkai Kaiho 2005; 108:1144-51. [PMID: 16440811]
28. Chung SW, Chung HY, Toriba A, Kameda T, Tang N, Kizu R, Hayakawa K. An environmental quinoid polycyclic aromatic hydrocarbon, acenaphthenequinone, modulates cyclooxygenase-2 expression through reactive oxygen species generation and nuclear factor kappa B activation in A549 cells. Toxicol Sci 2007; 95:348-55. [PMID: 17082565]
29. Bedard K, Krause KH. The NOX family of ROS-generating NADPH oxidases: physiology and pathophysiology. Physiol Rev 2007; 87:245-313. [PMID: 17237347]
30. Hool LC, Di Maria CA, Viola HM, Arthur PG. Role of NAD(P)H oxidase in the regulation of cardiac L-type Ca2+ channel function during acute hypoxia. Cardiovasc Res 2005; 67:624-35. [PMID: 15913584]
31. Li Y, Trush MA. Diphenyleneiodonium, an NAD(P)H oxidase inhibitor, also potently inhibits mitochondrial reactive oxygen species production. Biochem Biophys Res Commun 1998; 253:295-9. [PMID: 9878531]
32. Stolk J, Hiltermann TJ, Dijkman JH, Verhoeven AJ. Characteristics of the inhibition of NADPH oxidase activation in neutrophils by apocynin, a methoxy-substituted catechol. Am J Respir Cell Mol Biol 1994; 11:95-102. [PMID: 8018341]
33. Inoguchi T, Sonta T, Tsubouchi H, Etoh T, Kakimoto M, Sonoda N, Sato N, Sekiguchi N, Kobayashi K, Sumimoto H, Utsumi H, Nawata H. Protein kinase C-dependent increase in reactive oxygen species (ROS) production in vascular tissues of diabetes: role of vascular NAD(P)H oxidase. J Am Soc Nephrol 2003; 14:S227-32. [PMID: 12874436]
34. Talior I, Tennenbaum T, Kuroki T, Eldar-Finkelman H. PKC-delta-dependent activation of oxidative stress in adipocytes of obese and insulin-resistant mice: role for NADPH oxidase. Am J Physiol Endocrinol Metab 2005; 288:E405-11. [PMID: 15507533]
35. Pinton P, Rimessi A, Marchi S, Orsini F, Migliaccio E, Giorgio M, Contursi C, Minucci S, Mantovani F, Wieckowski MR,

Del Sal G, Pelicci PG, Rizzuto R. Protein kinase C beta and prolyl isomerase 1 regulate mitochondrial effects of the life-span determinant p66Shc. Science 2007; 315:659-63. [PMID: 17272725]

36. Wang N, Chintala SK, Fini ME, Schuman JS. Ultrasound activates the TM ELAM-1/IL-1/NF-kappaB response: a potential mechanism for intraocular pressure reduction after phacoemulsification. Invest Ophthalmol Vis Sci 2003; 44:1977-81. [PMID: 12714632]

37. Liton PB, Luna C, Bodman M, Hong A, Epstein DL, Gonzalez P. Induction of IL-6 expression by mechanical stress in the trabecular meshwork. Biochem Biophys Res Commun 2005; 337:1229-36. [PMID: 16229816]

38. Liton PB, Luna C, Challa P, Epstein DL, Gonzalez P. Genome-wide expression profile of human trabecular meshwork cultured cells, nonglaucomatous and primary open angle glaucoma tissue. Mol Vis 2006; 12:774-90. [PMID: 16862071]

Articles are provided courtesy of Emory University and the Zhongshan Ophthalmic Center, Sun Yat-sen University, P.R. China. The print version of this article was created on 16 August 2011. This reflects all typographical corrections and errata to the article through that date. Details of any changes may be found in the online version of the article.